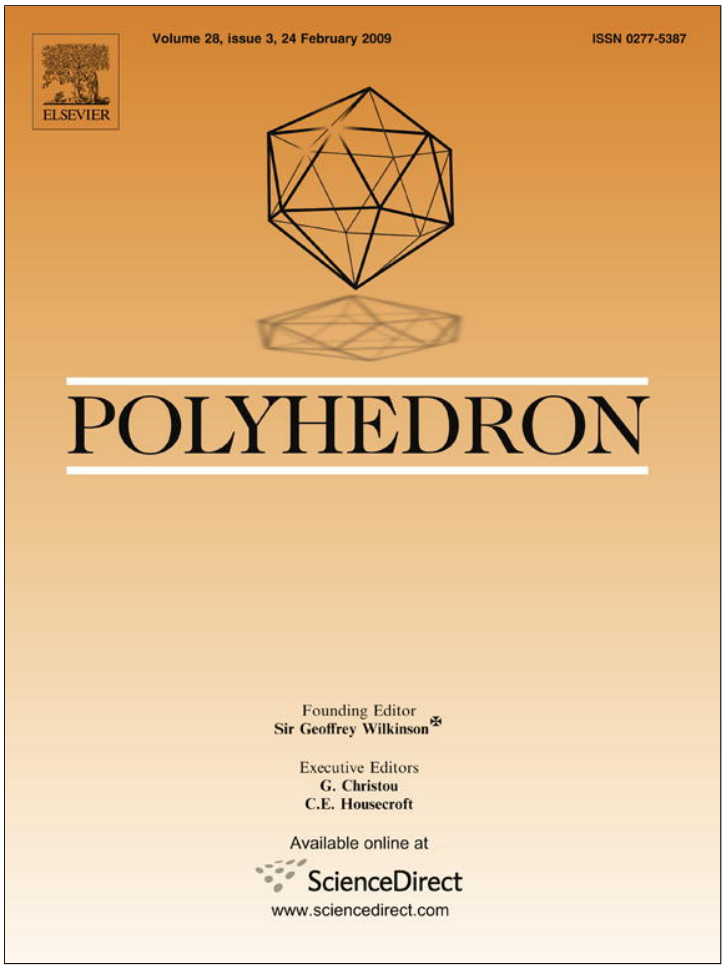

Polyhedron 28 (2009) 562–568

Contents lists available at ScienceDirect

Polyhedron

journal homepage: www.elsevier.com/locate/poly

# Synthesis and characterization of three novel molybdenum(VI) complexes: Mononuclear $[MoO_2(C_6H_4(O)CH{=}NCH(COO)CH_2C{=}(O)NH_2)]$, $[MoO_2(C_{19}H_{19}N_2O_5)(CH_3OH)]Cl \cdot CH_3OH$ and dinuclear $[Mo_2O_4(C_6H_4(O)CH{=}NCH(COO)CH_2C{=}(O)NH_2)_2]$

Marina Cindrić [a,*], Gordana Galin [a], Dubravka Matković-Čalogović [a], Predrag Novak [a], Tomica Hrenar [a], Ivan Ljubić [b], Tanja Kajfež Novak [a]

[a] Department of Chemistry, Faculty of Science, University of Zagreb, Horvatovac 102 a, 10001 Zagreb, Croatia
[b] Department of Physical Chemistry, Ruđer Bošković Institute, Bijenička Cesta 54, 10002 Zagreb, Croatia

ARTICLE INFO

*Article history:*
Received 16 June 2008
Accepted 20 November 2008
Available online 23 January 2009

*Keywords:*
Molybdenum chelates
N, O ligands
X-ray diffraction
NMR spectroscopy

ABSTRACT

The molybdenum(VI) complexes $[Mo_2O_4(C_6H_4(O)CH{=}NCH(COO)CH_2C{=}ONH_2)_2]$ (**1**), $[MoO_2(C_6H_4(O)CH{=}NCH(COO)CH_2C{=}(O)NH_2)]$ (**3**) and $[MoO_2(C_{19}H_{19}N_2O_5)(CH_3OH)]Cl \cdot CH_3OH$ (**4**), of salicylaldehyde amino acid derivatives (DL-asparagine or L-ornithine hydrochloride) have been synthesized and characterized. The Schiff base containing a saturated heterocyclic ring (in complex **4**) is the first example of such a molecule derived from salicylaldehyde and the amino acid, L-ornithine hydrochloride. We proposed that the formation of a molybdenum(VI) complex coordinated by a Schiff base containing a saturated heterocyclic ring depends upon the nature of the solvent and upon the presence of molybdenum(VI). In the absence of molybdenum(VI), the condensation product obtained from the reaction of L-ornithine hydrochloride and salicylaldehyde was the Schiff base *N*-salicylidene-L-ornithine (**5**). In the dinuclear complex **1** and the mononuclear complexes **3** and **4**, the molybdenum atoms are octahedrally coordinated with two *cis* oxo-oxygen atoms (in **3** and **4**), oxo-bridging atoms (in **1**) and the Schiff base ligand. In **3** the *N*-salicylidene-DL-asparaginato ligand coordinates molybdenum tetradentately while in **1** and **4** the Schiff base ligand acts as a tridentate ligand.



## 1. Introduction

During the last decade, intensive studies have been carried out on the biochemical, pharmacological and physicochemical functions of molybdenum. In particular, many kinds of dioxomolybdenum(VI) compounds have been synthesized as models of molybdoenzymes in order to study and elucidate catalytic oxygen atom transfer reactions [1–7]. For example, dioxomolybdenum(VI) complexes have been studied as models for oxidized forms of molybdoenzymes, e.g. aldehyde oxidase and sulfite oxidase which are supposed to contain *cis*-$MoOX_2$ units (X = O, S) coordinated to sulfur, nitrogen and oxygen donor atoms in the protein structure [4–7]. During the enzymatic turnover, the mononuclear molybdenum center is proposed to cycle between the IV and VI oxidation states, with the paramagnetic V state being the obligatory catalytic intermediate in the oxidative half-reaction of the enzyme. In the context of model systems for this type of reaction, a few studies have been concerned with the preparation and reactivity of molybdenum(VI) complexes of *N*-salicylidene-L-amino acids and their derivatives [8].

In the present work we describe products of the template synthesis of potentially tridentate and tetradentate Schiff base ligands, derived from salicylaldehyde (salH) and the amino acids DL-asparagine and L-ornithine hydrochloride, with the dioxomolybdenum(VI) core (Scheme 1).

Complex formation of $[MoO_2(sal)_2]$ with DL-asparagine and L-ornithine hydrochloride was studied in methanolic and dichloromethane solutions. The presence of mononuclear dioxomolybdenum(VI) centers in the complexes $[MoO_2(C_6H_4(O)CH{=}NCH(COO)CH_2C{=}(O)NH_2)]$ (**3**) and $[MoO_2(C_{19}H_{19}N_2O_4)(CH_3OH)]Cl \cdot CH_3OH$ (**4**) was confirmed by the crystal structure determinations, while the chemical structure of the complex $[Mo_2O_4(C_6H_4(O)CH{=}NCH(COO)CH_2C{=}(O)NH_2)_2]$ (**1**) was determined by NMR spectroscopy.

Computational studies were proved and were concerned with the role of the molybdenum atom in the cyclization of the Schiff base derived from L-ornithine hydrochloride and salicylaldehyde.

* Corresponding author. Tel.: +385 1 460 6351; fax: +385 1 460 6340.
*E-mail address:* marina@chem.pmf.hr (M. Cindrić).

0277-5387/$ - see front matter © 2008 Elsevier Ltd. All rights reserved.
doi:10.1016/j.poly.2008.11.058

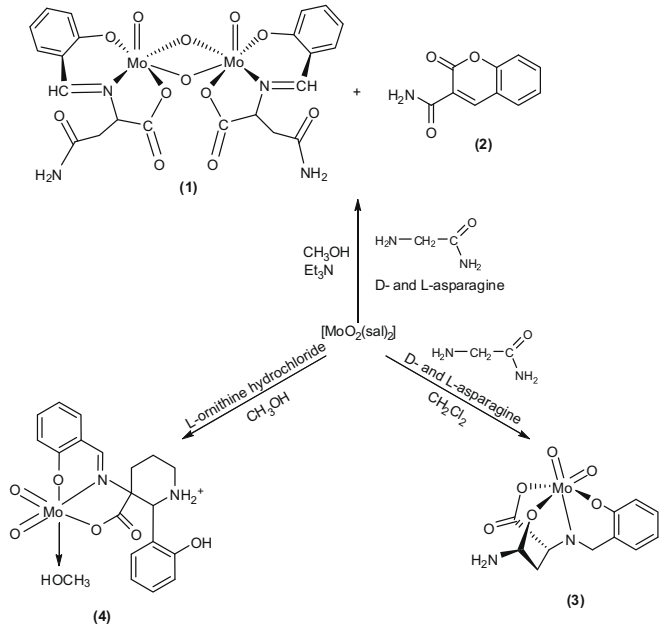


**Scheme 1.** Reactions of $[MoO_2(sal)_2]$ with D- and L-asparagine and L-ornithine hydrochloride.

## 2. Experimental

*Materials and methods:* L-Ornithine hydrochloride, DL-asparagine and triethylamine were of reagent grade and were used as purchased. Methanol was dried using magnesium turnings and iodine, and then distilled. Dichloromethane was dried over $P_2O_5$. The starting complex $[MoO_2(sal)_2]$ was prepared as described in the literature [9].

*IR spectra:* Infrared spectra were recorded in KBr with a Spectrum RX I spectrophotometer in the 4500–450 $cm^{-1}$ region.

*Elemental analyses:* The Analytical Services Laboratory of the Rudjer Bošković Institute provided C, H and N analyses. Molybdenum was determined according to the method described in the literature [10].

### 2.1. Syntheses of the molybdenum(VI) complexes

#### 2.1.1. Synthesis of di-μ-oxo-di(N-salicylidene-DL-asparaginato) dioxodimolybdenum(VI), $[Mo_2O_4(C_6H_4(O)CH{=}NCH(COO)CH_2C{=}(O)NH_2)_2]$ (**1**)

$[MoO_2(sal)_2]$ (0.63 g, 1.7 mmol) was dissolved in dry methanol (35 ml) and the solution was refluxed under an argon atmosphere for 15 min before addition of DL-asparagine (0.45 g, 3.4 mmol) and a few drops of triethylamine. The reaction mixture was refluxed under an argon atmosphere for 7 h. The color of the solution changed from pale yellow to red. The yellow crystalline product, (**1**), that formed after 7 h was filtered off, washed with cold methanol and dried in vacuo. Yield: 0.08 g (13%). After six weeks needle-like transparent crystals of coumarin-3-carboxamide (**2**) were obtained from the mother liquor at room temperature. Yield: 0.06 g (10%).

(**1**) *Anal.* Calc. for $C_{22}H_{20}Mo_2N_4O_{13}$: C, 35.69; H, 2.72; N, 7.57; Mo, 25.91. Found: C, 35.30; H, 2.75; N, 7.62; Mo, 26.30%. IR (KBr) $\nu/cm^{-1}$: 3382, 1716, 1680, 1610, 1556, 1472, 1414, 908, 944, 820, 762, 638.

(**2**) *Anal.* Calc. for $C_{10}H_7NO_3$: C, 63.53; H, 3.73; N, 7.41. Found: C, 63.55; H, 3.40; N, 7.39%. IR (KBr) $\nu/cm^{-1}$: 3390, 3146, 1714, 1564, 1388, 1162, 1008, 770, 618.

#### 2.1.2. Synthesis of cis-dioxo(N-salicylidene-DL-asparaginato) molybdenum(VI), $[MoO_2(C_6H_4(O)CH{=}NCH(COO)CH_2C{=}(O)NH_2)]$ (3)

$[MoO_2(sal)_2]$ (0.63 g, 1.7 mmol) was dissolved in dry dichloromethane (35 ml) and the solution was refluxed under an argon atmosphere for 15 min before addition of DL-asparagine (0.45 g, 3.4 mmol). The reaction mixture was refluxed under an argon atmosphere for 5 h. The color of the solution changed to yellow. The yellow crystalline product, (**3**), that formed after 5 h was filtered off, washed with cold dichloromethane and dried *in vacuo*. Yield: 0.1 g (16%).

*Anal.* Calc. for $C_{11}H_{10}MoN_2O_6$: C, 36.48; H, 2.78; N, 7.74; Mo, 26.49. Found: C, 36.59; H, 2.75; N, 7.52; Mo, 26.30%. IR (KBr) $\nu/cm^{-1}$: 3372, 1730, 1665, 1600, 1576, 1422, 1410, 928, 944.

#### 2.1.3. Synthesis of 3-[(2,5-salicylideneiminato)-2-(2-hydroxyphenyl) (piperidinum)-3-carboxylato)methanol dioxomolybdenum(VI)] chloride methanol, (1/1) $[MoO_2(C_{19}H_{19}N_2O_4)(CH_3OH)]Cl \cdot CH_3OH$ (**4**)

$[MoO_2(sal)_2]$ (0.15 g, 0.41 mmol) and L-ornithine hydrochloride (0.14 g, 0.83 mmol) were dissolved in dry methanol (35 ml). The mixture was refluxed for 5 h under an argon atmosphere. After a few days an unstable yellow-green crystalline product (**4**) was obtained. The product was filtered off, washed with cold methanol and dried *in vacuo* under an argon atmosphere. Yield: 0.1 g (42%).

*Anal.* Calc. for $C_{21}H_{27}ClMoN_2O_8$: C, 44.49; H, 4.80; N, 4.94; Cl, 6.25; Mo, 16.92. Found: C, 43.96; H, 4.56; N, 5.01; Cl, 6.20; Mo, 16.63%. IR (KBr) $\nu/cm^{-1}$: 3172, 3028, 2938, 1668, 1624, 1600, 1454, 1428, 934, 909.

#### 2.1.4. Synthesis of N-salicylidene-L-ornithine hydrochloride, $C_6H_4(OH)CH_2NHCH(COOH)(CH_2)_3NH_2{\cdot}HCl$ (**5**)

L-Ornithine hydrochloride (0.84 g, 5 mmol) was dissolved in potassium hydroxide solution (0.289 g KOH in 10 ml water) and added to salicylaldehyde (1.22 g, 10 mmol in 10 ml EtOH). The mixture was stirred under reflux for 1 h with the almost immediate appearance of a yellow product. It was filtered off, washed with cold ethanol and dried in vacuo. Yield: 0.84 g (61.83%).

(**5**) *Anal.* Calc. for $C_{12}H_{17}ClN_2O_3$: C, 52.85; H, 6.28; N, 10.27; Cl, 13.00. Found: C, 53.01; H, 6.10; N, 9.87; Cl, 12.65%. IR (KBr) $\nu/cm^{-1}$: 3050, 2948, 1638, 1582, 1514, 1410, 1338, 1284, 846, 750.

### 2.2. X-ray crystallography

Crystal parameters, data collection details and refinement results for compounds **3** and **4** are summarized in Table 1. Diffraction data for **3** were collected on an Oxford Diffraction Xcalibur 3 CCD diffractometer at 295 K, and those for **4** on an Enraf-Nonius Mach 2000 diffractometer at 110 K. Graphite-monochromated Mo Kα radiation ($\lambda = 0.71073$ Å) was used for both data collections. The data were corrected for Lorentz and polarization effects by CRYSALIS [11] and DENZO programs [12] for **3** and **4**, respectively. Both structures were solved by direct and Fourier methods using SHELXS-97 [13] and SHELXL-97 [14], respectively. They were refined by the full-matrix least-squares method based on $F^2$ values against all reflections assuming anisotropic temperature factors for all non-H atoms using the SHELXL-97 program integrated in the WINGX package [15]. All hydrogen atoms were found, however due to the somewhat poor geometry, those on carbon atoms were generated and left to ride on their parent atoms. The two amino-hydrogen atoms in **3** were refined isotropically. The positional parameters of the hydrogen atoms attached to the nitrogen and oxygen atoms in **4** were left as found in the difference Fourier map and only their isotropic thermal parameter was refined. Figures were made with the programs ORTEP [16] and PLATON [17].

**Table 1**
General and crystal data, summary of intensity data collection and structure refinement for compounds **3** and **4**.

| | **3** | **4** |
|---|---|---|
| Formula | $C_{11}H_{10}MoN_2O_6$ | $C_{21}H_{27}ClMoN_2O_8$ |
| Formula weight | 362.15 | 566.84 |
| Color | yellow | yellow-green |
| Temperature (K) | 293(2) | 110(2) |
| Wavelength (Å) | 0.71073 | 0.71073 |
| Crystal system | monoclinic | triclinic |
| Space group | $P2_1/a$ | $P\bar{1}$ |
| *Unit cell parameters* | | |
| $a$ (Å) | 12.059(2) | 9.6417(19) |
| $b$ (Å) | 7.364(3) | 10.134(2) |
| $c$ (Å) | 15.329(3) | 12.701(3) |
| $\alpha$ (°) | 90 | 79.83(3) |
| $\beta$ (°) | 111.730(19) | 78.28(3) |
| $\gamma$ (°) | 90 | 78.09(3) |
| $V$ (Å$^3$) | 1264.5(6) | 1177.2(5) |
| $Z$ | 4 | 2 |
| $\rho_{calc}$ (g cm$^{-3}$) | 1.902 | 1.599 |
| $F(000)$ | 720 | 580 |
| Crystal size (mm$^3$) | 0.31 × 0.11 × 0.07 | 0.25 × 0.20 × 0.17 |
| $\theta$ range for data collection (°) | 4.3–29.5 | 3.5–28.3 |
| No. of measured reflections | 14209 | 10712 |
| No. of independent reflections [$R_{int}$] | 3484 [0.0495] | 5812 [0.0133] |
| No. of observed reflections, $I \geq 2\sigma(I)$ | 2390 | 5296 |
| No. parameters | 189 | 306 |
| Absorption correction | integration | integration |
| $\mu$ (mm$^{-1}$) | 1.065 | 0.720 |
| Range of transmission factors | 0.825, 0.913 | 0.822, 0.863 |
| $R$[a], $wR$[b] [$I \geq 2\sigma(I)$] | 0.0508, 0.1419 | 0.0243, 0.0579 |
| $R$, $wR$ (all data) | 0.0708, 0.1572 | 0.0281, 0.0595 |
| $g_1$, $g_2$ in $w$[c] | 0.0921, 0 | 0.0186, 0.7504 |
| Goodness-of-fit on $F^2$, S[d] | 1.110 | 1.075 |
| Minimum and maximum electron density (e Å$^{-3}$) | −0.981, 1.724 | −0.486, 0.399 |

[a] $R = \sum||F_o| - |F_c||/\sum|F_o|$.
[b] $wR = [\sum(F_o^2 - F_c^2)^2/\sum w(F_o^2)^2]^{1/2}$.
[c] $w = 1/[\sigma^2(F_o^2) + |g_1P + g_2P|$ where $P = (F_o^2 + 2F_c^2)/3$.
[d] $S = \sum[w(F_o^2 - F_c^2)^2/(N_{obs} - N_{param})]^{1/2}$.

### 2.3. NMR measurements

One and two-dimensional NMR spectra were recorded on Bruker Avance DRX500 and Bruker Avance DPX 300 spectrometers equipped with a 5 mm diameter inverse detection probe and a 5 mm $^1H/^{13}C$ dual probe, respectively, and $z$-gradient accessory. TMS was used as the internal standard. Standard spectral conditions were used for the $^1H$ and $^{13}C$ (PENDANT) NMR experiments. The sample concentration was 20 mg ml$^{-1}$ in [$D_6$]DMSO solutions. The digital resolution was 0.1 and 0.3 Hz per point for $^1H$ and $^{13}C$ spectra, respectively. COSY spectra were recorded with spectral width of 4000 Hz in each domain and with 1024 points in the f2 dimension. A 2s relaxation delay was used to acquire 512 increments for each data set. Free induction decays were processed using a 2K × 1K matrix with appropriate zero filling and sine weighting. The digital resolution was 3.9 and 15.6 Hz per point in the f2 and f1 dimensions, respectively. The HSQC and HMBC spectra were recorded with a relaxation delay of 1.5 s and 32 scans per increment. The spectral width was 31 000 Hz in acquisition domain f2 and 4000 Hz in time domain f1. Data were collected into a 2048 × 512 acquisition matrix and processed using a 2K × 1K transformed matrix with zero filling in the f1 domain. Sine multiplication was performed before Fourier transformations. In HMBC spectra the delay for long-range couplings was set to 60 ms.

### 2.4. Computational details

In all calculations we consistently used the same generalized gradient (GGA) corrections in determining the self-consistent charge density and the exchange-correlation (XC) part of the energy corresponding to the charge density. The used functional was the recently proposed OPBE [18], which combines the OPTX exchange devised by Handy and Cohen [19] with the correlation term proposed by Perdew et al. [20]. The local density approximation (LDA) part was based upon the Vosko–Wilk–Nusair (VWN) [21] parameterization of electron gas. The relativistic effects were accounted for via the scalar zeroth order regular approximation (ZORA) formalism [22], which was employed throughout. We made use of a basis set built from Slater type functions (STOs) and tailored especially for the ZORA approach, as reflected by the use of much steeper functions in the core region. The basis set consisted of a TZP quality set on the Mo atom with all the orbitals up to, and including 3d treated as a frozen core, DZP sets on the C, N and O atoms with the 1s orbital frozen, and a DZP set on the H atoms. In [$MoO_2(C_{19}H_{19}N_2O_4)$] (the complex cation of **4** without coordinated and solvated methanol molecules) there thus resulted a total of 473 symmetrized fragment orbitals. The recommended sets of auxiliary fit functions to facilitate computations of the Coulomb potential were employed unchanged. All the DFT calculations were performed using the ADF program system [23].

## 3. Results and discussion

### 3.1. Synthesis of the complexes

The yellow dinuclear molybdenum(VI) complex [$Mo_2O_4$-($C_6H_4$(O)CH=NCH(COO)$CH_2$C=(O)$NH_2$)$_2$] (**1**) and coumarin-3-carboxamide $C_{10}H_7NO_3$ (**2**) were obtained by the reaction of [$MoO_2$(sal)$_2$] and DL-asparagine in dry methanol under an argon atmosphere. Cavaco et al. isolated coumarin 3-carboxamide and the vanadium(IV) complex [VO(sal-L-asn)(py)($H_2O$)] in the reaction of $VOSO_4$, salicylaldehyde and L-asparagine, and they proposed a mechanism of oxidative decarboxylation of L-asparagine [24]. These reactions of biochemical and chemical decarboxylation of α-amino acids activated by metal ions are well documented [25–27].

The compounds **1** and **2** were characterized by IR spectra and the chemical structure of compound **1** was determined by the combined use of one- and two-dimensional NMR spectroscopy. The NMR results for compound **2** were in accordance with the literature data [24]. The proton and carbon chemical shifts of **1** are displayed in Table 2.

The two amide protons in **1** were readily assigned in the proton spectrum since their signals disappeared after the addition of $D_2O$ owing to a rapid proton/deuterium exchange. Also the HMBC spectrum revealed connectivities from these protons to the C(11) carbonyl carbon. The HMBC correlation peak between one of the amide protons and C(10) was further established. In addition, the imino proton H(7) showed connectivities to C(2), C(3) and C(1) in the aromatic ring and to C(8) which was further correlated to

**Table 2**
$^1H$ and $^{13}C$ chemical shifts (ppm) of **1**.

| Atom (compound **1**) | $^1H$ | $^{13}C$ |
|---|---|---|
| 1 | | 159.74 |
| 2 | | 121.53 |
| 3 | 7.67 | 134.79 |
| 4 | 7.11 | 121.34 |
| 5 | 7.61 | 135.99 |
| 6 | 6.99 | 118.55 |
| 7 | 8.76 | 164.89 |
| 8 | 4.92 | 65.91 |
| 9 | – | 174.67 |
| 10 | 2.93 | 39.21 |
| 11 | | 170.79 |
| $NH_2$ | 7.34, 7.31 | |

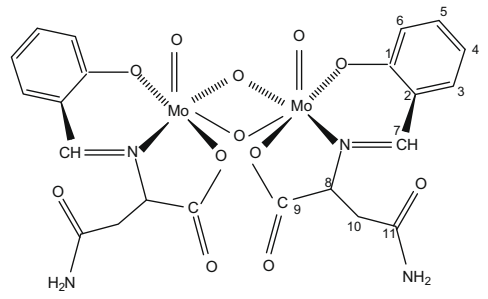

**Scheme 2.** $[Mo_2O_4(C_6H_4(O)CH{=}NCH(COO)CH_2C{=}(O)NH_2)_2]$ (**1**).

H(10). HMBC correlation peaks between H(8) and C(9) and C(11) were also observed corroborating the structure depicted in Scheme 2.

In the IR spectrum of compound **1**, the strong absorption bands at 820 $cm^{-1}$ and in the region 908–944 $cm^{-1}$ were assigned to the bridging and terminal Mo–O groups of the $Mo_2O_4^{4+}$ core and are in accordance to the literature data for the same type of complexes [28].

The mononuclear molybdenum(VI) complex, $[MoO_2(C_6H_4(O)CH{=}NCH(COO)CH_2C{=}(O)NH_2)]$ (**3**) was obtained by the reaction of $[MoO_2(sal)_2]$ and DL-asparagine in dry dichloromethane under an argon atmosphere. In the dinuclear **1** and mononuclear **3** complexes, molybdenum is coordinated by the deprotonated tridentate ONO (in **1**) and tetradentate OONO (in **3**) *N*-salicylidene-DL-asparaginato ligand. The coordination sphere in **1** is completed by one oxo-oxygen and two oxo-bridging atoms, and in **3** by two *cis* oxo-oxygen atoms.

The mononuclear molybdenum(VI) complex $[MoO_2(C_6H_4(O)CH{=}NC_5H_7(COO)NH_2C_6H_4(O)(CH_3OH)]Cl \cdot CH_3OH$ (**4**) was obtained in the reaction of $[MoO_2(sal)_2]$ and L-ornithine hydrochloride in dry methanol under an argon atmosphere (Scheme 3). We were able to isolate complex **4** from the methanolic solution, however the same reaction in dichloromethane (with or without addition of triethylamine) was unsuccessful.

Since L-ornithine contains an additional side-chain amino group we expected the formation of a molybdenum(VI) complex coordinated by a *bis*-Schiff base such as $[MoO_2C_6H_4(O)CH{=}NCH(COOH)(CH_2)_3N{=}CH(O)C_6H_4]$. However, X-ray investigations showed that in the obtained molybdenum(VI) complex, the molybdenum atom is coordinated by a Schiff base containing a saturated heterocyclic ring. According to the literature data [29] such Schiff base ligands are formed from the condensation reaction of 2-pyridinecarboxaldehyde derivatives with certain polyamines. Different metal salts (e.g. Fe(II), Ni(II), Zn(II)) have been reported to yield complexes of the corresponding Schiff base obtained in the condensation reaction of 2-pyridinecarboxaldehyde and α,ω-triamines [30].

In absence of molybdenum(VI) the condensation product obtained from the reaction of L-ornithine hydrochloride and salicylaldehyde in a 1:2 molar ratio was the Schiff base *N*-salicylidene-L-ornithine hydrochloride, $C_6H_4(OH)CH_2NHCH(COOH)(CH_2)_3NH_2 \cdot HCl$.

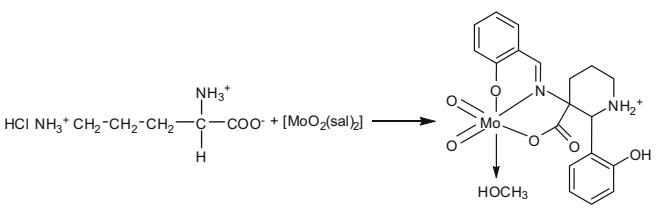

**Scheme 3.** Molybdenum(VI) coordinated by a Schiff base containing a saturated heterocyclic ring.

The IR spectra of all the described molybdenum(VI) complexes showed characteristic vibrations for this type of compound and the data are in accordance with that in the literature [28]. Complexes **3** and **4** underwent a rapid decomposition when dissolved in DMSO–$d_6$ and they were found to be insoluble in other solvents.

### 3.2. Structural studies

#### 3.2.1. Structures of $[MoO_2(C_6H_4(O)CH{=}NCH(COO)CH_2C{=}(O)NH_2)]$ (3) and $[MoO_2(C_{19}H_{19}N_2O_5)(CH_3OH)]Cl \cdot CH_3OH$ (4)

In both structures the main feature is the mononuclear, octahedrally coordinated molybdenum atom with two *cis* oxo-oxygen atoms and a bound Schiff base ligand. In **3** the *N*-salicylidene-DL-asparaginato ligand coordinates molybdenum tetradentately (Fig. 1), while in **4** (2,5-salicylideneiminato)-2-(2-hydroxophenyl)(piperidinum)-3-carboxylate acts as a tridentate ligand. The coordination sphere in **4** is completed by a methanol molecule (Fig. 2). Selected bond distances and angles are presented in Table 3 for both structures.

Distortion from an ideal octahedral geometry is more pronounced in **3** with the acute angle N(1)–Mo–O(6) of 70.40(8)°, obtuse angle O(1)–Mo–O(2) of 105.96(15)° closed by two *cis* oxo-oxygen atoms, and the *trans* chelating angle O(2)–Mo–N(1) of 150.92(11)°. This is caused by more strain imposed by the rigid geometry of the tetradentate Schiff base ligand in **3**. The greatest distortion from the octahedral geometry in **4** is that of the *trans* chelating angle O(3)–Mo–O(4) of 151.07(5)°. An analysis was carried out on structures deposited with the Cambridge Structural Database [31] by defining an octahedrally coordinated mononuclear molybdenum atom, a Schiff base *N*-donor, three single bonded oxygen atoms and two *cis* oxo-oxygen atoms. The search gave 55 hits. The Mo=O bond is the shortest, with a mean value of 1.701(1) Å. The mean Mo–O bond that is *trans* to the Mo–O single bond is 1.945(4) Å (Mo–O range 1.887–2.025 Å, O–Mo–O range 147.4–158°), whereas the one *trans* to the oxo-oxygen atom is lengthened due to the *trans*-influence and amounts to 2.334(6) Å (Mo–O range 2.171–2.416 Å, O=Mo–O range 160.7–175.6°). The lengths of the Mo–O(1) and Mo–O(2) bonds in both structures are within the normal range for typical *cis*-$MoO_2$ structures. The coordinating oxygen atoms O(3) and O(5) of the Schiff base ligand are *trans* to each other and their distance to Mo is close to the mean value from the CSD. The Mo–O(6) bond in **3** exhibits a *trans*-influence and is significantly longer than the two unaffected bonds mentioned above. This bond length is comparable to those found in the complexes $[MoO_2L(ROH)]$ (L = tridentate Schiff bases derived

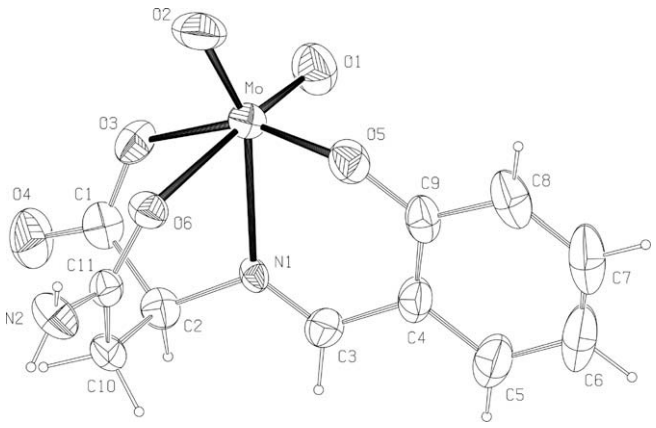

**Fig. 1.** ORTEP projection of **3** with ellipsoids at the 50% probability level.

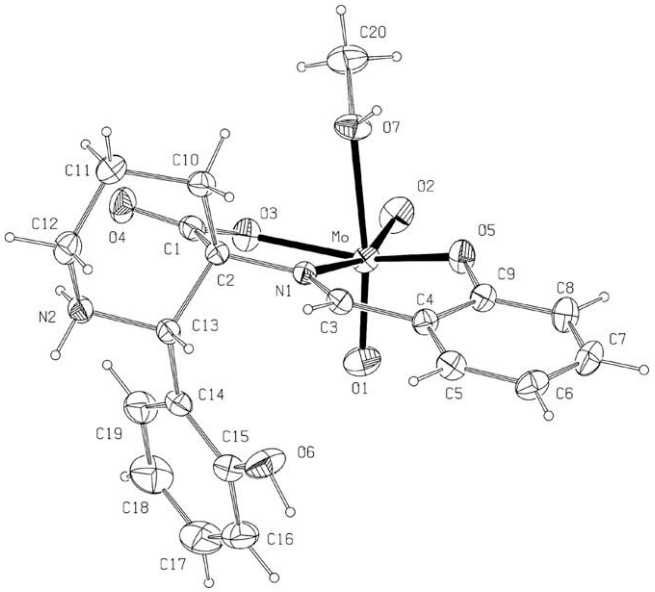


**Fig. 2.** ORTEP projection of **4** with ellipsoids at the 50% probability level.

**Table 3**
Selected bond distances (Å) and angles (°) for compounds **3** and **4**.

| Distances (Å) | 3 | 4 | Angles (°) | 3 | 4 |
|---|---|---|---|---|---|
| Mo–O(1) | 1.679(3) | 1.6985(14) | O(1)–Mo–O(2) | 105.96(15) | 104.99(7) |
| Mo–O(2) | 1.701(3) | 1.6964(13) | O(1)–Mo–O(3) | 94.52(13) | 97.51(6) |
| Mo–O(3) | 2.023(3) | 2.0243(14) | O(1)–Mo–O(5 | 97.61(14) | 99.63(7) |
| Mo–O(5) | 1.937(3) | 1.9140(13) | O(1)–Mo–O(6) | 171.91(13) | 169.71(6) |
| Mo–O(6)[a] | 2.351(2) | 2.2925(14) | O(1)–Mo–N(1) | 102.52(13) | 93.62(6) |
| Mo–N(1) | 2.253(3) | 2.2510(14) | O(2)–Mo–O(3) | 97.34(14) | 94.75(6) |
| C(1)–O(3) | 1.297(5) | 1.295(2) | O(2)–Mo–O(5) | 101.10(15) | 103.05(6) |
| C(1)–O(4) | 1.210(4) | 1.222(2) | O(2)–Mo–O(6)[a] | 80.77(12) | 84.12(6) |
| C(1)–C(2) | 1.524(5) | 1.535(2) | O(2)–Mo–N(1) | 150.92(11) | 159.28(6) |
| C(2)–N(1) | 1.465(4) | 1.479(2) | O(3)–Mo–O(5) | 154.16(14) | 151.07(5) |
| C(3)–N(1) | 1.243(4) | 1.288(2) | O(3)–Mo–O(6)[a] | 79.97(11) | 76.64(5) |
| C(3)–C(4) | 1.458(5) | 1.445(2) | O(3)–Mo–N(1) | 74.50(10) | 73.48(5) |
| C(9)–O(5) | 1.347(5) | 1.3502(19) | O(5)–Mo–N(1) | 80.62(11) | 82.31(5) |
| | | | O(5)–Mo–O(6)[a] | 85.27(11) | 82.63(6) |
| | | | N(1)–Mo–O(6)[a] | 70.40(8) | 76.67(5) |

[a] Symmetry transformation used to generate equivalent atoms: $-x, -y, -z$.

from salicylaldehyde or 2-hydroxy-1-naphthaldehyde and 2-(hydroxymethyl)aniline or 2-aminoethanol; R = $CH_3$ or $C_2H_5$) [32] and [$MoO_2$LD] (L = tridentate Schiff bases derived from 2-hydroxy-1-naphthaldehyde or 2-hydroxy-3-methoxybenzaldehyde and 2-amino-*p*-cresol; D = methanol, ethanol, DMSO, imidazole or 4,4′-bipyridine) [33]. A CSD search similar to the one described above was carried out, this time defining that the single bonded oxygen atom in the *trans* position to the oxo-oxygen is from methanol. This search gave 20 hits with a Mo–O mean distance of 2.357(7) Å (range 2.311–2.414 Å, O═Mo–O range 165.8–173.2°). The methanol oxygen atom O(7) is *trans* to the terminal oxo-group in **4** and is at 2.2925(14) Å from Mo. It is the shortest bond of that kind found so far. Only one Mo–$OCH_3$ bond is shorter but it is from a binuclear complex in which the methoxo group bridges two molybdenum atoms [34]. In the 55 structures from the CSD, the imine nitrogen is always *trans* to the terminal oxo-oxygen with a mean value of the Mo–N distance of 2.272(5) Å (range 2.202–2.413 Å, N–Mo═O 156.1–168.6°). The Mo–N(1) distance is similar in **3** and **4** (2.253(3) and 2.2510(14) Å, respectively) and slightly shorter than the mean value. It is similar to that in [$MoO_2$(L)(D)] (L = tridentate Schiff baze, D = azole ligand) [35]. The C(3)–N(1) bond distance is close to the usual C═N bond length [33,36]. The

**Table 4**
Hydrogen bond geometry (distances (Å), angles (°)) in **3**.

| D–H···A | D–H | H···A | D···A | D–H···A |
|---|---|---|---|---|
| N(2)–H(21)···O(3)[i] | 0.79(5) | 2.31(5) | 3.043(5) | 153(5) |
| N(2)–H(22)···O(6)[ii] | 0.75(6) | 2.23(6) | 2.932(5) | 158(5) |
| C(10)–H(10A)···O(2)[iii] | 0.97 | 2.53 | 3.336(5) | 141 |
| C(10)–H(10B)···O(6)[ii] | 0.97 | 2.53 | 3.451(2) | 159 |
| C(3)–H(3)···O(2)[iii] | 0.93 | 2.51 | 3.396(2) | 159 |

Symmetry transformations used to generate equivalent atoms: (i) $-1/2 - x, 1/2 + y, -z$; (ii) $-x, 1 - y, -z$; (iii) $x, 1 + y, z$.

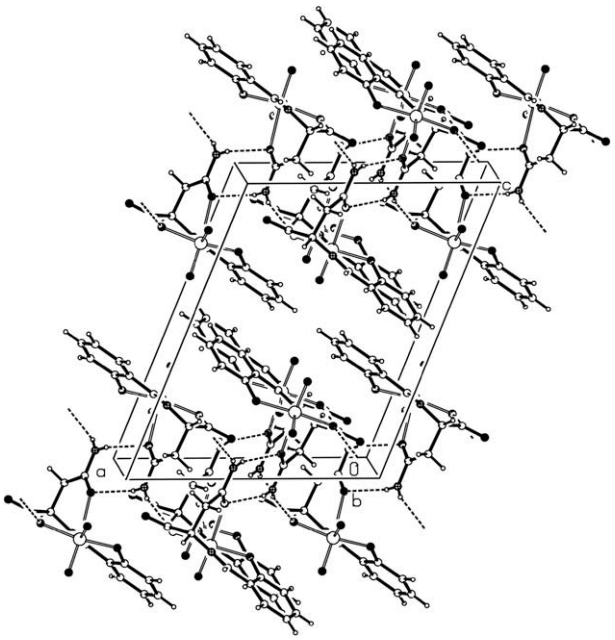

**Fig. 3.** Packing of **3** in the unit cell. Hydrogen bonds are shown by dashed lines.

angle between the planes of the two chelate rings Mo–O(3)–C(1)–C(2)–N(1) and Mo–O(5)–C(9)–C(4)–C(3)–N(1) is 11.28(6) and 17.72(14)° in **3** and **4**, respectively. Two centrosymmetrical hydrogen bonds of the type N–H···O (Table 4, Fig. 3) interconnect each molecule of **3** to two neighboring ones, thus forming infinite chains along [100].

In **4** a network of hydrogen bonds interconnects the complex cation, chloride anion and the methanol solvent molecule (Fig. 4, Table 5). One hydrogen atom of the non-coordinating N(2) atom in the piperidinium ring is linked by intra- and intermolecular hydrogen bonds to the carboxylic oxygen atom O(6) at 2.880(2) and 2.871(2) Å, respectively, while the other hydrogen atom forms an intermolecular hydrogen bond to the chloride ion at 3.0389(17) Å. The oxygen atom of the methanol molecule O(8) is linked by two hydrogen bonds, as an acceptor from the hydroxo group of the 2-hydroxophenolic ring O(5) at 2.647(2) Å, and as a donor toward the oxo-oxygen atom O(1) at 2.858(2) Å. The coordinating methanol ligand forms a hydrogen bond with the chloride ion. The crystal structure is additionally stabilized by weak C–H···O hydrogen bonds in the range 3.288(2)–3.670(2) Å.

### 3.3. Computational studies

Computational studies were primarily concerned with the role of the molybdenum atom in the cyclization step, which connects the reactant **R** with product **P** (Figs. 2 and 5). The latter is essentially equivalent to complex **4**, apart from the omission of the solvent $CH_3OH$ molecule from the Mo coordination sphere. As the

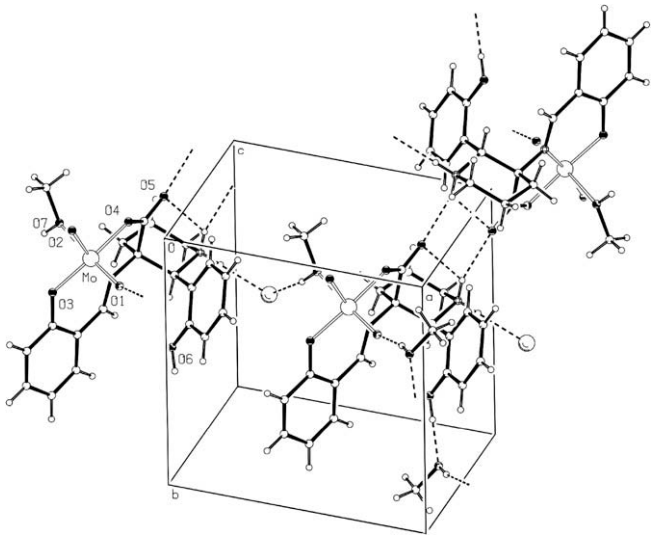


**Fig. 4.** Complex cation, chloride anion and methanol molecule of **4** interconnected by hydrogen bonds (shown by dashed lines).

**Table 5**
Hydrogen bond geometry (distances (Å), angles (°)) in **4**.

| D–H···A | D–H | H···A | D···A | D–H···A |
|---|---|---|---|---|
| N(2)–H(2[a])···O(4) | 0.85 | 2.29 | 2.880(2) | 127 |
| N(2)–H(2[a])···O(4)[i] | 0.85 | 2.12 | 2.871(2) | 146 |
| N(2)–H(2B)···Cl[ii] | 0.88 | 2.17 | 3.0389(17) | 169 |
| O(6)–H(6[a])···O(8)[iii] | 0.92 | 1.74 | 2.647(2) | 171 |
| O(7)–H(71)···Cl | 0.91 | 2.05 | 2.9527(15) | 168 |
| O(8)–H(8[a])···O(1)[iv] | 0.88 | 1.99 | 2.858(2) | 169 |
| C(3)–H(3)···Cl[iii] | 0.93 | 2.63 | 3.5436(19) | 167 |
| C(10)–H(10[a])···Cl[iii] | 0.97 | 2.83 | 3.670(2) | 146 |
| C(6)–H(6)···O(2)[v] | 0.93 | 2.51 | 3.396(2) | 159 |
| C(7)–H(7)···O(2)[vi] | 0.93 | 2.57 | 3.288(2) | 135 |

[a] Symmetry transformations used to generate equivalent atoms: (i) 2−*x*, −*y*, 1 − *z*; (ii) 1 + *x*, *y*, *z*; (iii) 1 − *x*, 1 − *y*, 1 − *z*; (iv) −1 + *x*, *y*, 1 + *z*; (v) *x*, 1 + *y*, *z*; (vi) 1 − *x*, 1−*y*, −*z*.

most demanding test of accuracy of the current theoretical approach, the calculated distances of the Mo–ligand bonds in **P**, as well as the torsional angles within the $MoO_2$ containing ring, are compared to the experimental ones in Table 6.

The **P** complex is 2.8 kcal mol$^{-1}$ less stable than **R**, which is not much considering the unfavorable steric interactions arising in **P**, where the 6-membered heterocyclic ring has to accommodate the two very large substituents in a vicinal position (Fig. 5).

To get a better understanding of the role of the Mo atom in the cyclization process, reference test compounds were devised by substituting $MoO_2$ with a $CH_2$ group. These are labelled as P($CH_2$) and R($CH_2$) in analogy with the parent compounds. The energy difference between P($CH_2$) and R($CH_2$) now increases to 6.7 kcal mol$^{-1}$. More importantly, substantial differences are observed between the $MoO_2$ and $CH_2$ containing rings. The former is much less puckered owing to the additional Mo binding to the imine N(1), which makes the ring more rigid, thus restricting its conformational mobility. As a result, the steric repulsions are less pronounced in P than in P($CH_2$). Still, it seems that the reaction involving the $CH_2$ substituted compounds would proceed as well, albeit with much more difficulty.

The basic assumptions about the mechanism include the activation of C(2) as a nucleophile, which is achievable either *via* abstraction of the attached H atom by a base (whereby a carbanion is formed), or via a keto-enol tautomerism. With regards to the tautomerism, the energy difference between the keto and enol form in R is 16.3 kcal mol$^{-1}$, being in favor of the former form. This however is much less than that for R($CH_2$), where the difference equals 26.4 kcal mol$^{-1}$. The calculated Hirshfeld charges [37] concerned the trends in the charge re-distribution on going from the keto to the enol tautomeric form in R and R($CH_2$). The main differences may be summarized in the O(4) atom, which upon enolization passes considerably more (by ca. 0.05e) of its negative charge in R than in R($CH_2$). One small part of it (ca. 0.01e) is received by the Mo atom, however, most importantly the C(3) atom (Fig. 2) receives a major part (0.06e) of the charge in R, whereas in R($CH_2$) the equivalent atom receives effectively none. In the enol forms, C(1) of R($CH_2$) gets notably richer (by ca. 0.05e) than in R, while negligible differences between R and R($CH_2$) upon the charge redistribution are found only for the C(2) and N(1) atoms. The near flatness of the $MoO_2$ containing ring (Table 6) brings about a much more effective delocalization of the charge via resonance effects, all the way to C(3). Thus, R is much better adapted to the emergence of the double C(1)=C(2) bond of the enol form than R($CH_2$). An alternative route of activating the C(2) atom via H transfer to the vicinal imine N(1) is highly unlikely. In this case, upon protonation, N(1) rapidly escapes the Mo coordination sphere, which severely distorts the $MoO_2$ containing ring and destabilizes the structure by several 10s of kcal mol$^{-1}$. Similarly, the N(2) Schiff base is itself far too weak to directly deprotonate the C(2) atom. Indicative of this are the very high energies (around 60 kcal mol$^{-1}$ above **R**) when the proton is moved away from C(2) toward N(2). According to our calculations, yet another prerequisite for the cyclization to occur involves H transfer from O(6) to the imine N(2), whereby the electrophilicity of the vicinal C(13) is enhanced, making it much more prone to attack by the nucleophilic C(2), which completes the cyclization. The structures with the H atom on O(6) and N(2) are effectively isoenergetic, the energy difference being only 2.9 kcal mol$^{-1}$ in favor of the structure with the protonated O(6). The corresponding H bond is a very strong one, around 15 kcal mol$^{-1}$. Similar activation steps involving H transfer from

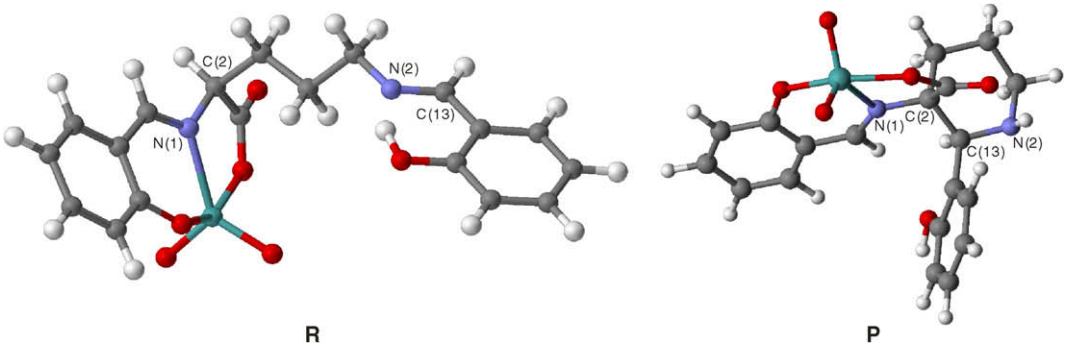


**Fig. 5.** Optimized structures of reactant **R** and product **P**.

**Table 6**
Selected structural parameters for complex **4** (product **P**) (distances in Å and torsional angles in °).

| Geometrical parameter | OPBE/TZ2P(DZP) | Experimental |
|---|---|---|
| r[Mo–N(1)] | 2.237 | 2.251(1) |
| r[Mo–O(1)] | 1.699 | 1.699(1) |
| r[Mo–O(2)] | 1.698 | 1.696(1) |
| r[Mo–O(3)] | 1.994 | 2.024(1) |
| r[Mo–O(5)] | 1.984 | 1.914(1) |
| τ[C(4)–C(9)–O(5)–Mo] | −27.9 | −32.8(2) |
| τ[C(9)–C(4)–C(3)–N(1)] | 10.7 | 13.5(3) |
| τ[C(4)–C(3)–N(1)–C(2)] | −175.2 | −178.4(2) |
| τ[C(3)–N(1)–C(2)–C(1)] | −157.4 | −175.5(1) |
| τ[C(2)–C(1)–O(3)–Mo] | 3.8 | −9.6(2) |

an OH group to a nearby Schiff base have been discovered several times in the past [38].

Finally, the mutual approach of the C(2) and C(13) reaction centers is easily achieved owing to the mobility of the aliphatic $–(CH_2)_3–$ chain, e.g. the conformations of **R** likely to precede the cyclization are less than 10 kcal $mol^{-1}$ above the most stable conformer of **R**. In the Supplementary movie it is seen that the reaction proceeds without a barrier once the C(2) and C(13) are separated by ca. 2.5 Å, and the enol and N(2) protonated forms are realized. Simultaneously as the C(2)–C(13) bond is formed, the proton attached to O(4) is smoothly abstracted by the N(2) atom, thus restoring the carbonyl bond. At the end a zwitterionic species is formed with the positive ammonium and negative phenolate parts. Additional calculations confirmed this zwitterionic form as unstable, with the proton eventually returning from N(2) to the O(6) atom. In conclusion, the formation of the tautomeric enol form (nucleophilic activation of C(2)) accompanied by the H transfer from O(6) to N(2) (electrophilic activation of C(13)) are the most probable initiation steps under the experimental conditions ($CH_3OH$ as the solvent). By far the largest barrier is expected for the keto-enol tautomerism, which is therefore the most likely candidate for the rate-determining step.

## 4. Conclusions

In this study it was shown that the *N*-salicylidene-DL-asparaginato anion coordinates to molybdenum(VI) as a tridentate OON (in **1**) or a tetradentate OONO (in **4**) ligand, depending on the reaction conditions (solvent). The coumarine-3-carboxamide (**2**) was obtained as a product of decarboxylation of DL-asparagine in methanolic solution and in the presence of molybdenum(VI). The reaction of L-ornithine hydrochloride and the salicylaldehydato molybdenum(VI) complex in methanol resulted in a mononuclear molybdenum(VI) complex (**4**) coordinated by a Schiff base containing a saturated heterocyclic ring. The presence of molybdenum(VI) and methanol as the solvent were important for obtaining this type of complex.

## Acknowledgments

We thank Prof. Boris Kamenar and Dr. sc. Višnja Vrdoljak, Assist. Prof., for useful discussions. Financial support for this research was provided by the Ministry of Science and Technology of the Republic of Croatia (Grant Nos. 119-1101342-1082, 119-1191342-1083, 119-1193079-1084, 119-1191342-2959, 098-0982915-2944).

## Appendix A. Supplementary data

CCDC 652690 and 652691 contain the supplementary crystallographic data for complexes **3** and **4**, respectively. These data can be obtained free of charge via http://www.ccdc.cam.ac.uk/conts/retrieving.html, or from the Cambridge Crystallographic Data Centre, 12 Union Road, Cambridge CB2 1EZ, UK; fax: (+44) 1223-336-033; or e-mail: deposit@ccdc.cam.ac.uk. Supplementary data associated with this article can be found, in the online version, at doi:10.1016/j.poly.2008.11.058.

## References

[1] C.G. Young, A.G. Wedd, Chem. Commun. (1997) 1251.
[2] L.F. Veiros, A. Prazers, P.J. Costa, C.C. Romao, F.E. Kuhn, M.J. Calhorda, J. Chem. Soc., Dalton Trans. (2006) 1383.
[3] R.R. Mendel, J. Chem., Dalton Trans. (2005) 3404.
[4] R. Hill, Chem. Rev. 96 (7) (1996) 2757.
[5] B.E. Schultz, S.F. Gheller, M.C. Muetterties, M.J. Scott, R.H. Holm, J. Am. Chem. Soc. 115 (1993) 2714.
[6] F.E. Inscore, S.Z. Knottenbelt, N.D. Rubie, H.K. Joshi, M.L. Kirk, J.H. Enemark, Inorg. Chem. 45 (2006) 967.
[7] R.J. Greenwood, G.L. Wilson, J.R. Pilbrow, A.G. Wedd, J. Am. Chem. Soc. 115 (1993) 5385.
[8] L. Casella, M. Gullotti, A. Pintar, Inorg. Chim. Acta 144 (1988) 89.
[9] K. Yamanuochi, S. Yamada, Inorg. Chim. Acta 9 (1974) 83.
[10] G.A. Parker, Analytical Chemistry of Molybdenum, Springer-Verlag, New York, 1983, p. 29.
[11] CRYSALIS Software system, Version 1.170, Xcalibur CCD system, Oxford Diffraction Ltd., 2003.
[12] Z. Otwinowski, W. Minor, DENZO-SCALEPACK, processing of X-ray diffraction data collected in oscillation mode, in: C.W. Carter Jr., R.M. Sweet (Eds.), Methods in Enzymology, Vol. 276: Macromolecular Crystallography, Part A, Academic Press, 1997, p. 307.
[13] G.M., Sheldrick, SHELXS-97, Program for Crystal Structure Solution, University of Göttingen, Germany, 1997.
[14] G.M. Sheldrick, SHELXL-97, Program for the Refinement of Crystal Structures, University of Göttingen, Germany, 1997.
[15] L.J. Farrugia, J. Appl. Crystallogr. 32 (1999) 837.
[16] L.J. Farrugia, ORTEP3 for windows, J. Appl. Crystallogr. 30 (1997) 565.
[17] (a) A.L. Spek, PLATON, A Multipurpose Crystallographic Tool, Utrecht University: Utrecht, The Netherlands, 1998;
(b) A.L. Spek, Acta Crystallogr., Sect A 46 (1990) C34.
[18] M. Swart, A.W. Ehlers, K. Lammertsma, Mol. Phys. 102 (2004) 2467.
[19] N.C. Handy, A. Cohen, J. Mol. Phys. 99 (2001) 403.
[20] J.P. Perdew, K. Burke, M. Ernzerhof, Phys. Rev. Lett. 77 (1996) 3865.
[21] S.H. Vosko, L. Wilk, M. Nusair, Can. J. Phys. 58 (1980) 1200.
[22] (a) E. van Lenthe, J.G. Snijders, E.J. Baerends, J. Chem. Phys. 105 (1996) 6505; (b) E. van Lenthe, A.E. Ehlers, E.J. Baerends, J. Chem. Phys. 110 (1999) 8943.
[23] (a) E.J. Baerends, J. Autschbach, A. Bérces, C. Bo, P.M. Boerrigter, L. Cavallo, D.P. Chong, L. Deng, R.M. Dickson, D.E. Ellis, L. Fan, T.H. Fischer, C.F. Guerra, S.J.A. van Gisbergen, J.A. Groeneveld, O.V. mGritsenko, M. Grüning, F.E. Harris, P. van den Hoek, H. Jacobsen, G. van Kessel, F. Kootstra, E. van Lenthe, D.A. McCormack, V.P. Osinga, S. Patchkovskii, P.H.T. Philipsen, D. Post, C.C. Pye, W. Ravenek, P. Ros, P.R.T. Schipper, G. Schreckenbach, J.G. Snijders, M. Sola, M. Swart, D. Swerhone, G. te Velde, P. Vernooijs, L. Versluis, O. Visser, E. van Wezenbeek, G. Wiesenekker, S.K. Wolff, T.K. Woo, T. Ziegler, ADF 2005.01 Release, SCM, Theoretical Chemistry, Vrije Universiteit, Amsterdam, <http://www.scm.com>; (b) G. te Velde, F.M. Bickelhaupt, S.J.A. van Gisbergen, C.F. Guerra, E.J. Baerends, J.G. Snijders, T. Ziegler, J. Comput. Chem. 22 (2001) 931
[24] I. Cavaco, J.C. Pessoa, M.T. Duarte, R.D. Gillard, P. Matias, Chem. Commun. (1996) 1365.
[25] M.C. Pirrung, J. Cao, J. Chen, Chem. Biol. 5 (1998) 49.
[26] S. Goldstein, G. Czapski, H. Choen, D. Meyerstein, R. van Eldik, Inorg. Chem. 33 (1994) 3255.
[27] W. Bal, M.I. Djuran, D.W. Margerum, E.T. Gray Jr., M.A. Mazid, R.T. Tom, E. Nieboer, P.J. Sadler, J. Chem. Soc., Chem. Commun. (1994) 1889.
[28] A. Syamal, M.R. Maurya, Synth. React. Inorg. Met.-Org. Chem. 16 (1986) 857.
[29] M. Boča, D. Valigura, W. Linert, Tetrahedron 56 (2000) 441.
[30] N. Brefuel, C. Lepetit, S. Shova, F. Dahan, J.-P. Tuchagues, Inorg. Chem. 44 (2005) 8916.
[31] (a) Cambridge Structural Database, V5.28, Cambridge Crystallographic Data Centre, 12 Union Road, Cambridge, England, 2006; (b) F.H. Allen, The Cambridge structural database: a quarter of a million crystal structures and rising, Acta Crystallogr. B58 (2002) 380.
[32] M. Cindrić, N. Strukan, V. Vrdoljak, T. Kajfež, B. Kamenar, Z. Anorg. Allg. Chem. 628 (2002) 2113.
[33] M. Cindrić, N. Strukan, V. Vrdoljak, B. Kamenar, Z. Anorg. Allg. Chem. 630 (2004) 585.
[34] X. Xu, X. Wang, H. Liu, X. You, J. Chem. Soc., Dalton Trans. (1993) 1377.
[35] C. Zhang, G. Rheinwald, V. Lozan, B. Wu, P.-G. Lassahn, H. Lang, C. Janiak, Z. Anorg. Allg. Chem. 628 (2002) 1259.
[36] A. Rana, R. Dindo, P. Sengupta, S. Ghosh, L.R. Falvello, Polyhedron 21 (2002) 1023.
[37] F.L. Hirshfeld, Theor. Chim. Acta 44 (1977) 129.
[38] (a) H. Merz, G. Zundel, Biochem. Biophys. Res. Commun. 138 (1986) 819; (b) C. Ögretir, D. Hakan, H. Berber, F.F. Taktak, J. Chem. Eng. Data 51 (2006) 46.